Carbohydrate Polymers 78 (2009) 945–952

Contents lists available at ScienceDirect

Carbohydrate Polymers

journal homepage: www.elsevier.com/locate/carbpol

Mucoadhesive property and biocompatibility of methylated *N*-aryl chitosan derivatives

Warayuth Sajomsang *, Uracha Rungsardthong Ruktanonchai, Pattarapond Gonil, Onanong Nuchuchua

National Nanotechnology Center, Nanodelivery System Laboratory, National Science and Technology Development Agency, Thailand Science Park, Pathumthani 12120, Thailand

ARTICLE INFO

Article history:
Received 4 June 2009
Received in revised form 2 July 2009
Accepted 10 July 2009
Available online 16 July 2009

Keywords:
Chitosan
Methylated *N*-aryl chitosan derivatives
Mucoadhesive property
Cytotoxicity

ABSTRACT

The methylated *N*-aryl chitosan derivatives, methylated *N*-(4-*N*,*N*-dimethylaminocinnamyl) chitosan chloride (MDMCMCh) and methylated *N*-(4-pyridylmethyl) chitosan chloride (MPyMeCh), were synthesized by two steps, the reductive amination and the methylation. The physicochemical properties of chitosan derivatives were determined by ATR-FTIR, NMR, X-ray diffraction (XRD) and thermogravimetric (TG) techniques. The XRD analysis showed that the crystallinity and thermal stability of methylated chitosan derivatives were lower than those of chitosan. The effects of degree of quaternization (DQ), polymer structure and positive charge location on mucoadhesive property and cytotoxicity were investigated by using a mucin particle method and MTT assay compared to *N*,*N*,*N*-trimethylammonium chitosan chloride (TMChC). It was found that the mucoadhesive property and cytotoxicity increased with increasing DQ. At the DQ of 65%, the mucoadhesive property of the MDMCMCh was twofold lower than that of the TMChC. However, this phenomenon did not affect the mucoadhesive property when the DQ was higher than 65%. Surprisingly, the MPyMeCh showed the lowest toxicity even with the high DQ. These could be due to the resonance effect of the positive charge in the pyridine ring and the molecular weight after methylation. Finally, our result revealed that the mucoadhesive property was dependent on the DQ and polymer structure whereas the cytotoxicity was dependent on the combination of the polymer structure, positive charge location and molecular weight after methylation.

© 2009 Elsevier Ltd. All rights reserved.

1. Introduction

Mucus is a viscoelastic gel layer which is located on the surface of the gastrointestinal, respiratory, urogenital, and eye tissues, as well as the peritoneal surface of intra-abdominal organs in human being and most animals. Mucus composes primarily of crosslinked, bundled, and entangled mucin fibers secreted by both goblet cells and the seromucinous glands of the lamina propria at the apical epithelium (Lai, Wang, Wirtz, & Hanes, 2009). Mucin fibers, typically 10–40 MDa in size and 3–10 nm in diameter, are proteins glycosylated via proline, threonine, and/or serine residues by *O*-linked *N*-acetyl galactosamine as well as *N*-linked sulfate-bearing glycans. Most of the mucin glycoproteins have high sialic acid and sulfate content leading to a strongly negative surface charge (Lai et al., 2009; Shogren, Gerken, & Jentoft, 1989). Therefore, the cationic polymers can be absorbed on the mucus via electrostatic interaction. Several classes of polymers have been proposed as mucoadhesives due to their ability to interact physically and/or chemically with the mucus. Chitosan is a natural cationic polysaccharide derived from chitin by partial deacetylation with strong alkaline solutions. It consists of β-(1,4)-2-amino-2-deoxy-D-glucopyranose units (GlcN) and a small amount of 2-acetamido-2-deoxy-D-glucopyranose or *N*-acetyl-D-glucosamine (GlcNAc) residues. Chitosan has been reported to exhibit a great variety of useful biological properties due to its non-toxicity, biodegradability, and biocompatibility. However, its biological activities appear only in acidic medium because of its poor solubility in neutral and basic pH. *N*,*N*,*N*-Trimethylammonium chitosan chloride (TMChC) was one of the quaternized chitosan derivatives firstly synthesized by Muzzarelli and Tanfani (1985). The quaternization was based on nucleophilic substitution of the primary amino group on the C-2 position of chitosan with iodomethane in the presence of sodium iodide, sodium hydroxide and *N*-methylpyrrolidone. The TMChC has been widely used in many applications because it can be dissolved in water over a wide pH range. The mucoadhesive application is one of the interesting applications of the TMChC which have been reported by several research groups. Snyman, Hamman, and Kotze (2003) examined mucoadhesive interactions of the TMChC with different degree of quaternization (DQ). They demonstrated that the presence of quaternary ammonium groups was detrimental to mucoadhesion. The authors related this adverse effect to conformation changes in the TMChC. However, the opposite results have been reported by Sandri et al. (2005). Recently, Jintapattanakit, Mao, Kissel, and Junyaprasert (2008) found that mucoadhesive properties of the TMChC were influenced by the combination of

* Corresponding author. Tel.: +66 2 564 7100; fax: +66 2 564 6981.
E-mail address: warayuth@nanotec.or.th (W. Sajomsang).

0144-8617/$ - see front matter © 2009 Elsevier Ltd. All rights reserved.
doi:10.1016/j.carbpol.2009.07.020

positive charge density, steric hindrance of dimethyl groups on polymer and molecular weight. The TMChC with relatively high degree of dimethylation (DD) showed reduction in both mucoadhesion and cytotoxicity. Nevertheless, the influence of the DD was insignificant when the DQ of the TMChC was higher than 40% at which physicochemical properties and cytotoxicity were mainly dependent upon the DQ. The electrostatic interaction of the quaternary ammonium chitosan derivative with the negatively charged mucin was the main driving force for its strong mucosal adhesion. However, high positive charge density of the quaternary ammonium chitosan derivative showed high toxicity. Similar results had been found by Kean, Roth, and Thanou (2005) who showed that the cytotoxicity of the TMChC increased with increasing DQ.

In this study, other factors that affected to the mucoadhesive property and cytotoxicity, the positively charged location and the polymer structure were proposed. It is well known that polymer structure is a main factor influencing its physicochemical properties. Therefore, two quaternary ammonium chitosan containing aromatic moieties, methylated *N*-(4-*N*,*N*-dimethylaminocinnamyl) chitosan chloride (MDMCMCh) and methylated *N*-(4-pyridylmethyl) chitosan chloride (MPyMeCh) with various DQs were synthesized. The chemical structures of the MDMCMCh and MPyMeCh are shown in Fig. 1. The influence of the DQ, the positively charged location and the polymer structure on the mucoadhesive property and cytotoxicity was investigated by comparing to the TMChC. The mucoadhesion and the biocompatibility of all methylated chitosan derivatives were determined by a mucin particle method and MTT assay, respectively.

2. Experimental

2.1. Materials and reagents

Chitosan with an average molecular weight (M_w) of 276 kDa was purchased from Seafresh Chitosan (Lab) Co., Ltd. in Thailand. The degree of deacetylation (DDA) of chitosan was determined to be 94% by ^{1}H NMR spectroscopy (Lavertu et al., 2003). A dialysis tubing with M_w cut-off of 12,000–14,000 g/mol from Cellu Sep T4, Membrane Filtration Products, Inc. (Segiun, TX, USA), was used to purify all modified chitosan derivatives. 4-Dimethylaminocinnamaldehyde and 4-pyridinecarboxaldehyde were purchased from Fluka (Deisenhofen, Germany). Sodium cyanoborohydride, iodomethane, and 1-methyl-2-pyrrolidone were purchased from Acros Organics (Geel, Belgium). Sodium iodide was purchased from Carlo Erba Reagent (Italy), and all other reagents were distilled before use.

2.2. Instrumentation

ATR-FTIR spectra of chitosan and its derivatives were collected with the Nicolet 6700 FT-IR spectrometer (Thermo Fisher Scientific) by using high-performance diamond single-bounce ATR. In all cases spectra were collected using 32 scans with a resolution of 4 cm^{-1}. The ^{1}H NMR and ^{13}C CP/MAS spectra were measured on ADVANCE AV 500 MHz spectrometer and ADVANCE 300 MHz Digital NMR spectrometer (Bruker), respectively. The X-ray diffraction (XRD) patterns were obtained by JEOL JDX-3530 theta-2theta X-ray diffractometer (Aremco Products, Inc.) with CuKα radiation

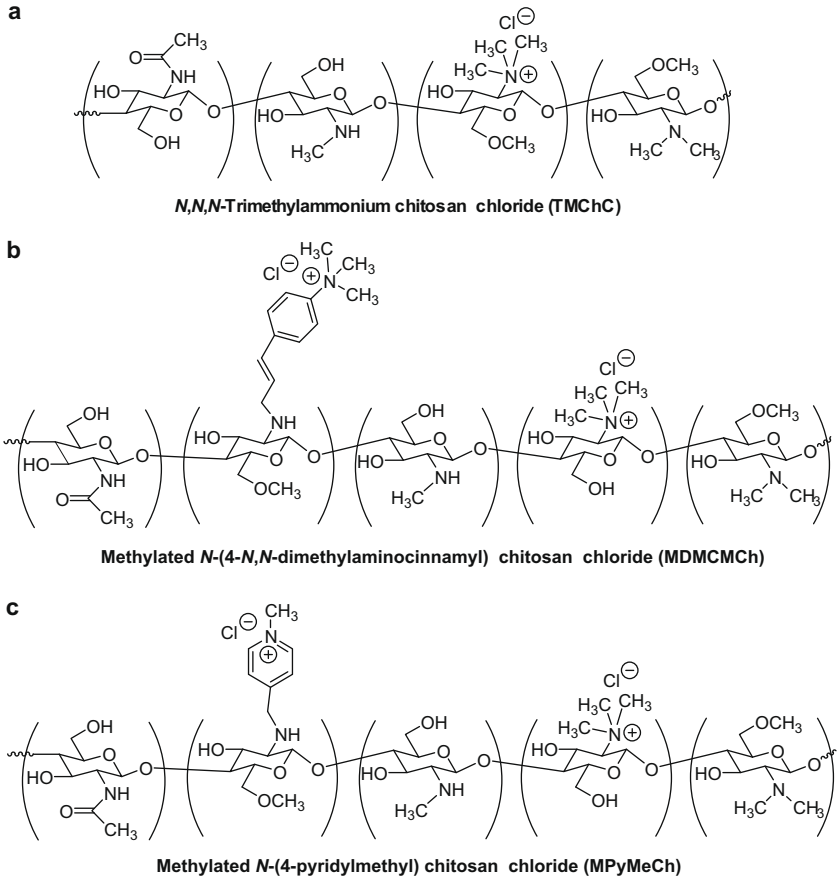

Fig. 1. Chemical structures of chitosan derivatives: (a) *N*,*N*,*N*-trimethyl chitosan chloride (TMChC), (b) methylated *N*-(4-*N*,*N*-dimethylaminocinnamyl) chitosan chloride (MDMCMCh) and (c) methylated *N*-(4-pyridylmethyl) chitosan chloride (MPyMeCh).

(λ = 0.154 nm). The 2θ angle was scaned between 5° and 50° at 25 °C. The voltage was 40 kV and the intensity was 50 mA. The thermogravimetric analysis (TGA) was recorded by TGA/SDTA 851 (METTLER TOLEDO) with a heating rate of 10 °C/min from 25 °C to 600 °C under nitrogen atmosphere.

2.3. Synthesis of the methylated N-aryl chitosan derivatives

The *N*-aryl chitosan derivatives were carried out in accordance with the previous reported procedure (Sajomsang, Gonil, & Saesoo, 2009) whereas the methylation of chitosan and *N*-aryl chitosan derivatives have been carried out by a single treatment with iodomethane in the presence of *N*-methyl pyrrolidone (NMP) and sodium hydroxide (Sajomsang, Tantayanon, Tangpasuthadol, & Daly, 2008).

2.4. Determination of the degree of N-substitution and the degree of quaternization

In this study, the degree of *N*-substitution (DS) and the degree of quaternization (DQ) were generally determined by using ^{1}H NMR spectroscopy as shown in Eqs. (1) (Crini et al., 1997) and (2), respectively (Polnok, Borchard, Verhoef, Sarisuta, & Junginger, 2004; Sieval et al., 1998). The degree of *N*,*N*-dimethylation (DD) and *O*-methylation (DOM) was determined by using Eqs. (3) and (4).

$$\text{DS}\ (\%) = (\text{Ar}/n)/[\text{H2} + 1/3\text{NHAc})] \times 100 \quad (1)$$

where DS (%) is the degree of *N*-substitution, Ar is the integral area of aromatic protons, *n* is the number of aromatic hydrogen atoms per substituent, H2 is the integral areas of the protons at C-2 carbon of GlcN, and NHAc is the integral area of GlcNAc protons.

$$\text{DQ}\ (\%) = (\text{N}^+(\text{CH}_3)_3/9)/\text{H1}' \quad (2)$$

$$\text{DD}\ (\%) = \text{N}(\text{CH}_3)_2/\text{H1}' \quad (3)$$

$$\text{DOM}\ (\%) = (\textit{O}\text{-CH}_3/3)/\text{H1}' \quad (4)$$

where DQ (%) is the degree of quaternization, the DQ at the primary amino groups of chitosan is denoted as DQ_{Ch}, DD (%) is the degree of *N*,*N*-dimethylation, DOM (%) is the degree of *O*-methylation, $N^+(CH_3)_3$ is the integral area of the *N*,*N*,*N*-trimethyl protons at δ 3.2 ppm, $N(CH_3)_2$ is the integral area of methyl protons at δ 2.7 ppm, *O*-CH_3 is the integral area of methoxy protons of either 3- or 6-hydroxy groups at δ 3.4 ppm or 3.3 ppm, respectively, and H1′ is the integral area of both H1′ and H1 protons in the range of δ 5.3–5.0 ppm.

2.5. Molecular weight determination

The weight average molecular weight (M_w), number average molecular weight (M_n), and M_w/M_n of chitosan and its derivatives were determined by using the gel permeation chromatography (GPC). The GPC consists of Waters 600E Series generic pump, injector, ultrahydrogel linear columns (M_w resolving range 1–20,000 kDa), guard column, pollulans as standard (M_w 5.9–788 kDa), and refractive index detector (RI). All samples were dissolved in acetate buffer pH 4 and then filtered through VertiPure nylon syringes filters 0.45 μm (VERTIC Vertical chromatography). The mobile phases, 0.5 M AcOH and 0.5 M AcONa (acetate buffer pH 4), were used at a flow rate of 0.6 mL/min at 30 °C. Then the injection volume 20 μL was used.

2.6. Estimation of water solubility

The water solubility of the MDMCMCh, MPyMeCh and TMChC with various pHs was estimated by using turbidity measurement. The test samples were dissolved in de-ionized water. Then 0.1 or 1 M HCl solution and 0.1 or 1.0 M NaOH solution were gradually added. The transmittance of the solution was recorded on a Lamda 650 UV/VIS Spectrophotometer (Perkin-Elmer) with an optical path length of 350 nm at 600 nm. The test was performed at 25 °C. All experiments were performed in triplicate.

2.7. Mucoadhesion by mucin particle method

Mucoadhesive properties of chitosan derivatives were determined by using the mucin particle method developed by Takeuchi et al. (2005). Submicron-sized mucin suspension (1% w/v) was prepared by suspending and continuously stirring mucin type III powder in Tris base pH 6.8 for 10 h. Mucin suspension was then incubated at 37 °C overnight. Then the size of mucin was reduced by ultrasonication (VCX750, Sonics & Materials, Inc.) until particle size was around 200–300 nm. It was then centrifuged at 4000 rpm for 20 min to extract submicron-sized mucin particles in the supernatant portion. The particle size and zeta-potential of the precisely size-controlled mucin particles were 250 ± 28 nm and −12.5 ± 1.6 mV, respectively.

One milliliter of 1% (w/v) mucin suspension was mixed with different concentrations of 0.05–0.5% (w/v) polymer solutions under mild magnetic stirring. The particle sizes and zeta-potential values were then measured by using photon correlation spectroscopy (NanoZS4700 nanoseries, Malvern Instruments) equipped with a 4 mW HeNe laser at a wavelength of 633 nm at 25 °C. The refractive index of chitosan derivatives and water were set at 1.33 and 1.33, respectively. All experiments were performed in triplicate.

2.8. Cytotoxicity testing by MTT assay

Skin fibroblast CRL 2076 cells were plated in 90 μL of Minimum Essential Medium (MEM) supplemented with 10% FBS at the density of 8000 cells/well in 96-well plates. When the cultures reached confluency, typically, 48 h after plating, all tested formulations at various concentrations were added at 10 μL/well. After 16 h post-incubation, 25 μL of 5 mg/mL MTT (3-(4,5-dimethyldiazol-2-yl)-2,5 diphenyl tetrazolium bromide) was added to each well and then incubated for another 4 h. Then, all media were removed and 100 μL of dimethyl sulfoxide was added. Plates were incubated for 30 min at 37 °C and the absorbance was measured at 550 nm by using a microplate reader. The percentage of cell viability values was then calculated and compared with the control samples. The IC_{50} was calculated as a polymer concentration which inhibited growth of 50% of cells relative to non-treated control cells.

3. Results and discussion

3.1. Synthesis of the methylated N-aryl chitosan derivatives

The *N*-(4-*N*,*N*-dimethylaminocinnamyl) chitosan (DMCMCh) and *N*-(4-pyridylmethyl) chitosan (PyMeCh) were carried out by reductive amination (Sajomsang et al., 2009). The DS of the DMCMCh and PyMeCh was in the range of 50–76% (Table 1). The methylation of the DMCMCh and PyMeCh was prepared by using iodomethane as methylating agent in the presence of NMP and sodium hydroxide. It was found that the DQ was in the range of 65% to 82% (Table 1). The methylation was occurred at both *N*,*N*-dimethylaminocinnamyl, *N*-pyridylmethyl moieties and the primary amino groups of chitosan. The result showed the reason why the

Table 1
Methylation of chitosan and *N*-aryl chitosan derivatives.

Samples	DS (%)	DQ_T (%)		DD (%)	DM (%)	Total *O*-CH_3 (%)	Recovery (%)
		DQ_{Ar} (%)	DQ_{Ch} (%)				
TMChC1	–	–	30	50	15	16	122
TMChC2	–	–	65	24	5	35	74
MDMCMCh1	50	50	15	24	–	15	90
MDMCMCh2	76	76	6	10	–	26	109
MPyMeCh1	52	52	18	12	5	23	80
MPyMeCh2	68	68	12	8	Trace	20	76

DS is the degree of *N*-substitution; DQ_{Ar} is the degree of quaternization at aromatic substituents; DQ_{Ch} is the degree of quaternization, DQ_T is the total degree of quaternization; DD is the degree of *N*,*N*-dimethylation; DM is the degree of *N*-methylation; Total *O*-CH_3 is the total degree of *O*-methylation of 3-*O* and 6-*O* at 3-hydroxyl and 6-hydroxyl positions of GlcN of chitosan, respectively; Recovery (%) is weight of product (g)/weight of starting reactant (g) × 100.

DQ of the methylated *N*-aryl chitosan derivatives was higher than that of the TMChC at the same condition. Besides quaternization, the *N*,*N*-dimethylation, *N*-methylation at the primary amino groups and *O*-methylation at the hydroxyl groups of chitosan were also occurred in the methylation process.

The ATR-FTIR and ^{1}H NMR spectroscopy were used to characterize the chemical structures of chitosan and its methylated derivatives in accordance with the previous report by our research group. The ATR-FTIR spectra of chitosan and its derivatives are shown in Fig. 2. The absorption bands at wavenumbers 1658, 1510 and 1570, 1469 cm^{-1} were assigned to the C=C stretching while the absorption band at wavenumbers 847 and 845 cm^{-1} were assigned to the C—H deformation (out of plane) of the aromatic groups for MDMCMCh and MPyMeCh, respectively. It is important to note both MDMCMCh and MPyMeCh exhibited the characteristic ATR-FTIR spectra at wavenumbers 1469 cm^{-1} due to C—H symmetric bending of the methyl substituent of quaternary ammonium groups (Sajomsang et al., 2009). From ATR-FTIR results, it was confirmed that the *N*-arylation and methylation of chitosan were successfully synthesized. The ^{1}H NMR spectra of the DMCMCh, PyMeCh, MDMCMCh and MPyMeCh were determined in accordance with the previous reported (Sajomsang et al., 2009). The DMCMCh exhibited a singlet proton signal at δ 3.1 ppm and the broad multiplet proton signals at δ 7.4 ppm, whereas the PyMeCh exhibited a doublet of doublets at δ 8.6–8.0 ppm. These protons were then assigned to the *N*,*N*-dimethyl protons at *para*-position of the aromatic group and the aromatic protons, respectively. The *N*,*N*,*N*-trimethyl protons signal of cinnamyl substituent was detected at δ 3.5 ppm while the methyl protons signal of pyridinum substituent was detected at δ 4.3 ppm. The protons signals at δ 3.2, 2.7 and 2.3 were assigned to the *N*,*N*,*N*-trimethyl protons, *N*,*N*-dimethyl protons, and *N*-methyl protons of GlcN, respectively. Furthermore, evidence of the *N*,*N*-dimethylaminocinnamyl carbons changed to the *N*,*N*,*N*-trimethylcinnamyl carbons was confirmed by CP/MAS ^{13}C NMR spectroscopy. Fig. 3 shows CP/MAS ^{13}C NMR spectra of the DMCMCh and MDMCMCh. It was found that the *N*,*N*-dimethylaminocinnamyl carbons at a chemical shift 41.2 ppm were observed in DMCMCh, whereas it does not detect the *N*,*N*-dimethylaminocinnamyl carbons signal in the MDMCMCh. Because the *N*,*N*-dimethylaminocinnamyl carbons were changed to the *N*,*N*,*N*-trimethylcinnamyl carbons during the methylation process, the *N*,*N*,*N*-trimethylcinnamyl carbons were detected at a chemical shift 58.3 ppm. It was confirmed that the *N*,*N*-dimethylaminocinnamyl substituent was completely methylated in this condition.

The weight average molecular weight (M_w), number average molecular weight (M_n) and M_w/M_n of chitosan and its derivatives were determined by gel permeation chromatography (GPC). The M_n, M_w and M_w/M_n of the chitosan were found as 48.71 kDa, 276.06 and M_w/M_n 5.67, respectively. A relatively wide molecular weight distribution with a polydispersity index (PDI) of chitosan was observed, which was similarly observed in case of the TMChC. It was noted that the lowest molecular weight of MPyMeCh (M_w 12–15 kDa) was obtained after methylation, compared to other methylated chitosan derivatives (Table 2). The methylation reaction led to a significant reduction in the chitosan molecular weight. It was plausible that an oxidative degradation process and alkaline depolymerization occurred.

3.2. X-ray diffraction

Fig. 4 shows the X-ray diffraction (XRD) patterns of chitosan and its derivatives. The XRD pattern of chitosan exhibited three characteristic peaks around 2θ = 11.2°, 20.8° and 22.9° (Zhang & Neau, 2001). The reflection fall at 2θ = 11.2° assigned to the crystal form I and the strongest reflection appeared at 2θ = 20.8° corresponding to crystal form II. Compared with chitosan, the broad single XRD patterns of the DMCMCh and MDMCMCh were observed at 2θ = 19.2° and 20.6°, respectively. The decrease in crystallinity of DMCMCh could be ascribed to the presence of 4-*N*,*N*-dimethylaminocinnamyl

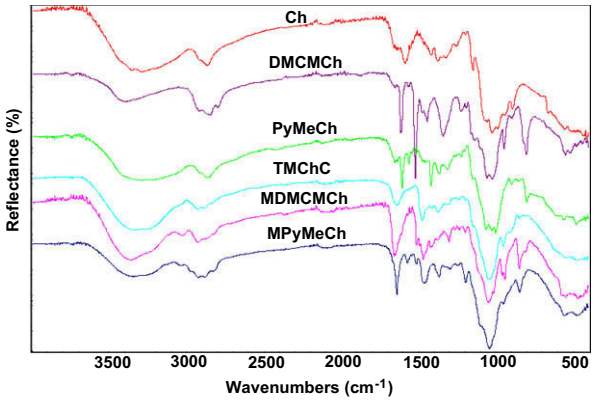

Fig. 2. ATR-FTIR spectra of chitosan (Ch), *N*-(4-*N*,*N*-dimethylaminocinnamyl) chitosan (DMCMCh), *N*-(4-pyridylmethyl) chitosan (PyMeCh), *N*,*N*,*N*-trimethyl chitosan chloride (TMChC), methylated *N*-(4-*N*,*N*-dimethylaminocinnamyl) chitosan chloride (MDMCMCh) and methylated *N*-(4-pyridylmethyl) chitosan chloride (MPyMeCh).

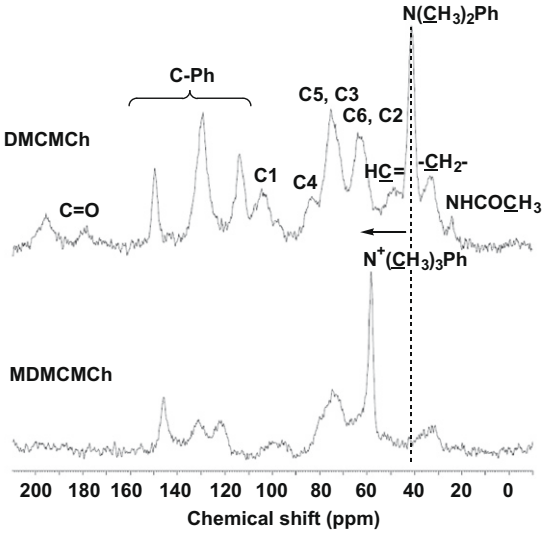

Fig. 3. CP/MAS ^{13}C NMR spectra of *N*-(4-*N*,*N*-dimethylaminocinnamyl) chitosan (DMCMCh) and methylated *N*-(4-*N*,*N*-dimethylcinnamyl) chitosan chloride (MDMCMCh).

Table 2
Characteristics of the interaction between mucin particle and methylated chitosan derivatives.

Samples	M_w (kDa)	DQ_T (%)	Equations	R^2	x% (w/v)
TMChC1	204.57	30	$y = -3.3714x + 1.6404$	0.9861	0.49
TMChC2	120.87	65	$y = -4.0029x + 0.966$	0.9731	0.24
MDMCMCh1	92.27	65	$y = -2.2134x + 1.0522$	0.9883	0.48
MDMCMCh2	40.35	82	$y = -4.3424x + 1.1048$	0.9737	0.25
MPyMeCh1	15.87	70	$y = -3.5927x + 0.8817$	0.9601	0.25
MPyMeCh2	12.22	80	$y = -3.6596x + 0.9186$	0.9569	0.25

x is the percentage of critical concentration (w/v).

moiety. This is possible that the steric hindrance of the 4-*N*,*N*-dimethylaminocinnamyl group obstructed the formation of inter- and extra-molecular hydrogen bonds of the chitosan backbone. Furthermore, it was also found that the crystallinity of the MDMCMCh was lower than that of the DMCMCh and chitosan. The low crystallinity of the MDMCMCh was resulted from the destruction of the strong hydrogen bonds in the parent chitosan. Therefore, the DMCMCh and MDMCMCh were amorphous more than chitosan. It was confirmed that the 4-*N*,*N*-dimethylaminocinnamyl moiety was successfully introduced into the chitosan backbone.

3.3. Thermogravimetric analysis

Thermogravimetric (TG) and derivative thermogravimetric (DTG) curves of chitosan and its derivatives are shown in Fig. 5. The thermograms of chitosan had two main decomposition stages. The first stage decomposed at 80 °C with weight loss about 11.6%, corresponding to water content in the chitosan backbone. The second stage started at 230 °C and reached the maximum of 306 °C. The weight loss was 54.7% due to the decomposition of chitosan backbone. The DMCMCh1 and DMCMCh2 showed three degradation stages. The first stage started at 54 °C and 51 °C with a weight loss of 5.0% and 2.2% ascribed to the volatile low molecular products and water content in the DMCMCh1 and DMCMCh2, respectively. The second and third degradation stages of the DMCMCh1 and DMCMCh2 started at 221 °C and 204 °C and then reached the maximum of 319 °C and 408 °C and 329 °C and 408 °C with a weight loss of 74.5% and 87.4%, respectively. The multiple steps of thermal degradation of the DMCMCh1 and DMCMCh2 were due to the degradation of the *N*,*N*-dimethylaminocinnamyl moiety. The MDMCMCh2 showed four degradation stages. The first stage started at 74 °C with a weight loss of 10.4% attributed to the water content. The second, third, and fourth degradation stages of the MDMCMCh2 started at 132 °C and then reached the maximum of 164 °C, 268 °C and 432 °C with a weight loss of 71.6%. These results indicated that the multiple steps of thermal degradation of the MDMCMCh2 were due to the degradation of the *N*,*N*,*N*-trimethylcinnamyl, *N*,*N*,*N*-trimethyl and *N*,*N*-dimethyl moieties. It is important to note that the water weight loss (%) of the DMCMCh was lower than that observed for chitosan. When increasing the DS, the percentage of water weight loss decreased. This was because of an increase in the hydrophobicity reduced the water absorption in the chitosan backbone (Sajomsang et al., 2008). On the other hand, the percentage of water weight loss increased in the MDMCMCh2 due to an increase in the hydrophilicity from quaternary ammonium moiety. Moreover, the chitosan had a high speed in decomposition between the temperature of 230 °C and 450 °C while the DMCMCh and MDMCMCh had a mild speed in decomposition during the temperature of 132–500 °C (Fig. 5a). The thermal stability of the DMCMCh and MDMCMCh was lower than that of the chitosan, but the scope of decomposition temperature was wider than that of chitosan. Furthermore, the onset of degradation temperature of the DMCMCh and MDMCMCh was shifted to lower temperature than that of the chitosan. This was attributed to a decrease in thermal stability as a consequence of an increase in the *N*,*N*-dimethylaminocinnamyl moiety and *N*,*N*,*N*-trimethylcinnamyl moiety. As the DS of the DMCMCh increased from 50% to 76%, the onset of degradation of DMCMCh showed a shift from 221 °C to 204 °C whereas the MDMCMCh had the onset of degradation at temperature 132 °C. This was indicated that the DMCMCh and MDMCMCh were less stable than the chitosan due to the weakness of inter- and extra-molecular hydrogen bonding.

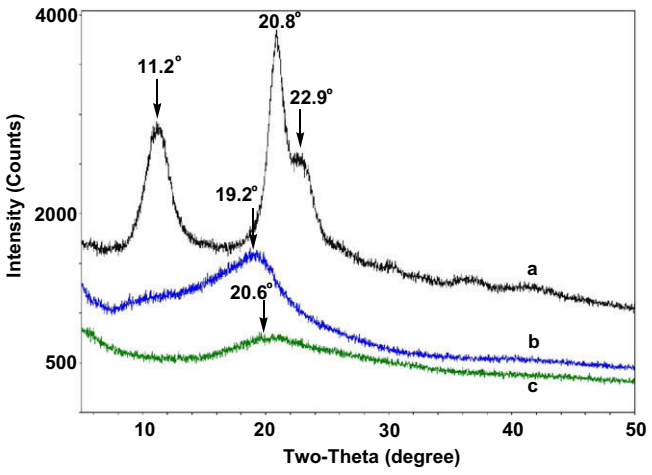

Fig. 4. X-ray diffraction patterns of chitosan, *N*-(4-*N*,*N*-dimethylaminocinnamyl) chitosan (DMCMCh) and methylated *N*-(4-*N*,*N*-dimethylcinnamyl) chitosan chloride (MDMCMCh).

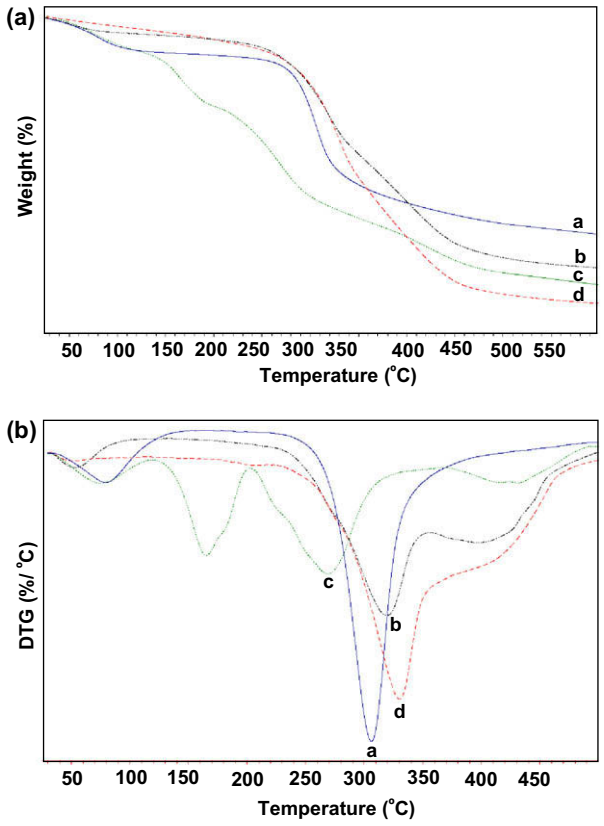

Fig. 5. Thermogravimetric (TG) (a) and derivative thermogravimetric (DTG) (b) thermograms of chitosan, *N*-(4-*N*,*N*-dimethylaminocinnamyl) chitosan (DMCMCh1 and DMCMCh2) and methylated *N*-(4-*N*,*N*-dimethylcinnamyl) chitosan chloride (MDMCMCh).

3.4. Water solubility

Fig. 6 exhibits the pH dependence of the transmittance of the MDMCMCh, MPyMeCh and TMChC with different DQ. The water solubilities of the MPyMeCh and TMChC2 were high and retained over a wide pH range, while the water solubilities of the TMChC1 and MDMCMCh were abruptly decreased in a basic pH. It was possible that the high hydrophobicity and the steric hindrance of *N*,*N*-dimethyl and *N*,*N*-dimethylaminocinnamyl moieties in the chitosan backbone might be decreased the water solubility. It was noted that the water solubilities of the MDMCMCh, MPyMeCh and TMChC were increased with increasing DQ. However, the water solubilities of the TMChC2 and MPyMeCh were not pH dependent.

3.5. Mucoadhesive property

The mucoadhesion of the methylated chitosan derivatives was investigated by commercially available porcine mucin particles at various amounts of polymer concentrations. In our study, we chose a commercial sample of lyophilised porcine mucin (type III). This product may differ slightly from the native porcine mucin because purification and storage may result in a partial degradation of glycoproteins and also in the formation of disulfide bridges due to oxidation of thiol groups in cysteine-rich subdomains (Sogias, Williams, & Khutoryanskiy, 2008). However, commercial mucin is often used in studies of mucoadhesion because it shows less batch-to-batch variability and gives more reproducible results (Rossi, Ferrari, Bonferoni, & Caramella, 2000, 2001). It was assumed that the surface property of the mucin particles would changed with an adhesion of the polymer if the polymer had a mucoadhesive property (Takeuchi et al., 2005). Fig. 7 shows an evolution of the particle size and zeta-potential of the mucin particles versus various methylated chitosan derivative concentrations. The zeta-potential of the mucin particles was a negative value before the mixing. By increasing an amount of the methylated chitosan derivatives, the zeta-potential of the mucin particles slowly changed from negative to positive values. The aggregation was occurred after the zeta-potential of the mucin exceeded the critical zeta-potential of the mucin (ca. −10 mV). Fig. 8 displays correlation between the zeta-potential of the methylated chitosan derivatives/mucin complexes (ZPv)/the zeta-potential of the starting mucin particles (ZP_0) ratios and the methylated chitosan derivative concentrations. The critical concentration value of their derivatives

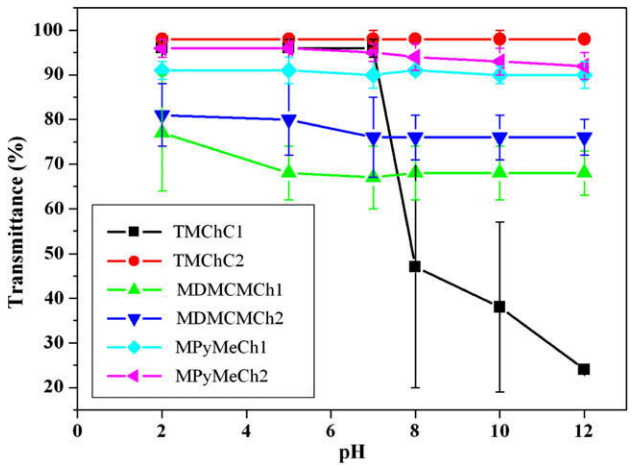

Fig. 6. The pH dependence of water solubility of *N*,*N*,*N*-trimethyl chitosan chloride (TMChC), methylated *N*-(4-*N*,*N*-dimethylaminocinnamyl) chitosan chloride (MDMCMCh) and methylated *N*-(4-pyridylmethyl) chitosan chloride (MPyMeCh) at 5 mg/mL.

was determined by a linear equation when ZPv/ZP_0 ratio equal to zero, suggesting that the mucin particles would be neutralized by an adsorption of the methylated chitosan derivative molecules on the surfaces (Table 2). The higher the concentration of the methylated chitosan derivatives, the more pronounced changes were found in zeta-potential. The stronger mucoadhesive bond strength, the higher value of slope as well as the lower critical concentration value were observed. It was found that the critical concentration values were in the range of 0.25–0.49% (w/v), whereas the slope values were in the range of −2.2 to −4.3. The mucoadhesive property increased with an increase in the DQ resulted in lower critical concentration values and higher slope values (Table 2 and Fig. 8). This result was in accordance with a report by Sandri et al. (2005). Moreover, Jintapattanakit et al. (2008) reported that besides the DQ, the DD was contributed to the mucoadhesive property. They also found that the mucoadhesive property of the TMChC linearly decreased with an increase in the ratio of the DD/DQ. It should be noted that at the same DQ level of 65%, the mucoadhesive property of the TMChC2 was twofold higher than that of the MDMCMCh1. The results could be explained in term of the electrostatic interaction between positively charged amino groups of the methylated chitosan and its methylated derivatives and the negatively charged sialic acid residue of mucus glycoproteins or mucins. An introduction of the *N*,*N*-dimethylaminocinnamyl moiety on the chitosan backbone reduced the interaction between polymer and mucin particles. Thus, the MDMCMCh1 had a lower mucoadhesive property than TMChC2. It could be possible that the steric hindrance of the *N*,*N*-dimethylaminocinnamyl group shielded the positive charges of the quaternary ammonium group on the GlcN of chitosan when the DQ was lower than 65%. This did not effect on mucoadhesive property when the DQ was higher than 65%. Furthermore, our investigation indicated that the interaction between mucin particles and the methylated chitosan derivatives was molecular weight-independence but it depended on the amount of charge density of the quaternary ammonium group. The result revealed that the MPyMeChs with DQ 70–80% had a mucoadhesive property as well as TMChC2 with DQ 65% even the molecular weight of the MPyMeChs was eightfold lower than that of TMChC2. However, the effect of chitosan molecular weight on the mucoadhesive property had been reported with various results and methods. Wang et al. (2007) studied the influence of molecular weight of chitosan (48, 124 and 230 kDa) to its mucoadhesive property by using UV spectrophotometry. They found that influence of chitosan molecular weight on mucoadhesion was not significant. Ferrari, Rossi, Bonferoni, Caramella, and Karlsen (1997) and Sandri et al. (2005) provided the same results which were the mucoadhesive property of chitosan or TMChC decreased with increasing the molecular weight. The method that they used was that tensile stress and rheological synergism methods. On the other hand, Jintapattanakit et al. (2008) found the interaction between the mucin particles and TMChC was molecular weight-dependent. The interaction decreased with decreasing molecular weight. This result was in accordance with a report by Qaqish and Amiji (1999) who found that the high molecular weight of chitosan had higher multivalent in association with the mucin particles than the low molecular weight. In addition, they used fluorescence polarization technique to characterize chitosan-mucin binding. The literature review results indicated that the effects of molecular weight on mucoadhesive property were still debatable. Thus, it needs further study.

3.6. Cytotoxicity

The effects of the positively charged location and the polymer structure on the skin fibroblast CRL 2076 cells were investigated by testing cell viability via MTT assay. Table 3 displays the concen-

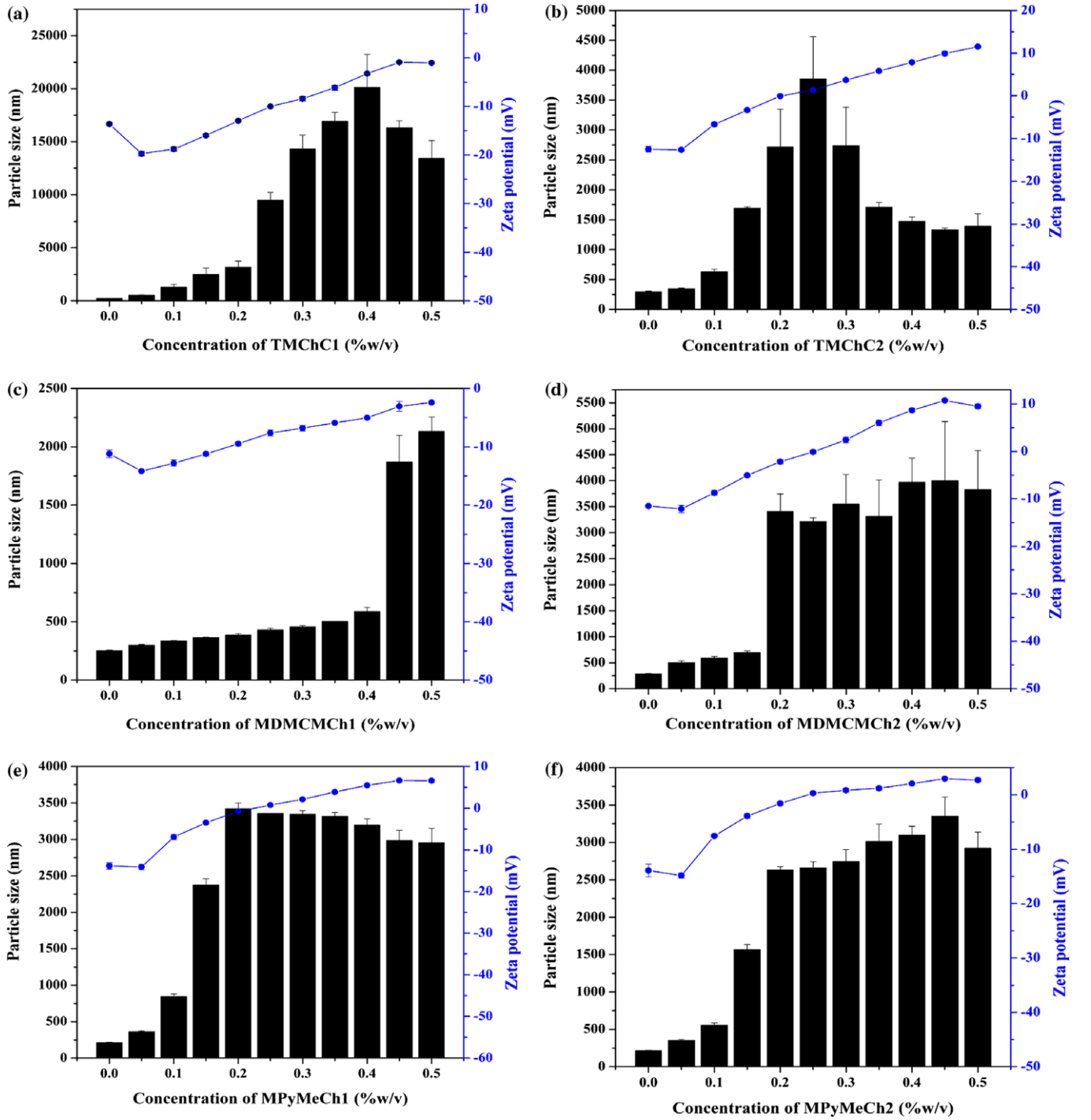

Fig. 7. The particle size (black bar) and zeta-potential (●) of the chitosan derivatives/mucin particles when mixed with the various concentrations of TMChC1 (a), TMChC2 (b), MDMCMChC1 (c), MDMCMChC2 (d), MPyMeCh1 (e) and MPyMeCh2 (f).

tration which inhibited 50% cell growth (IC_{50}) of the methylated chitosan derivatives with various DQs. The IC_{50} data showed that the DD/DQ ratio had considerable influence on the cytotoxicity. The lower IC_{50} value, the higher toxicity occurred. It was found that the cytotoxicity increased with decreasing DD/DQ ratio. The IC_{50} of the TMChC1 (DQ 30%) was higher than 500 μg/mL, whereas the TMChC2 (DQ 65%) was 14 μg/mL. This was similarly observed in the case of MDMCMCh. The MDMCMCh2 (DQ 82%) showed the highest cytotoxicity with the IC_{50} of 8 μg/mL. Regarding the effect of the DQ and DD, the cytotoxicity of TMChC and MDMCMCh began to increase when the DD/DQ ratio was lower than 1. This was in accordance to a report by Jintapattanakit et al. (2008). Moreover, they also found that the amount of methyl pendent groups from dimethylamino groups was insufficient to shield the positive charges of quaternary ammonium group when the DQ was higher than 40%, leading to low cell viability. However, the MPyMeCh1 and MPyMeCh2 exhibited the IC_{50} of 500 and 150 μg/mL even the DD/DQ ratio was lower than 1. Firstly, this could be due to the chemical structure of the MPyMeCh. Secondly, it could be due to the positively charged location. This was possible that the resonance effect of the positive charge in the pyridine ring would reduce the cytotoxicity. Finally, it could be due to the molecular

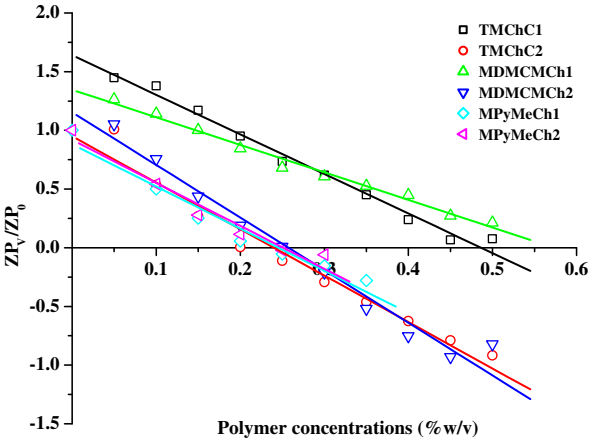

Fig. 8. Correlation between the polymer concentration and zeta-potential profile of the mucin/TMChC1 complexes (□), mucin/TMChC2 complexes (○), mucin/MDMCMCh1 complexes (△), mucin/MDMCMChC2 complexes (▽), mucin/MPyMeCh1 complexes (◇) and mucin/MPyMeCh2 complexes (◁).

Table 3
Cytoxicity of methylated chitosan derivatives on skin fibroblast CRL 2076 following 24 h incubation as determined by MTT assay ($n = 8$).

Samples	DS (%)	M_w (kDa)	DQ_{Ar} (%)	DQ_{Ch} (%)	DQ_T (%)	DD (%)	IC_{50} (μg/mL)
TMChC1	–	204.57	–	30	30	50	>500
TMChC2	–	120.87	–	65	65	24	14
MDMCMChC1	50	92.27	50	15	65	24	12
MDMCMChC2	76	40.35	76	6	82	10	8
MPyMeChC1	52	15.87	52	18	70	12	500
MPyMeChC2	68	12.22	68	12	80	8	150

weight of the MPyMeCh after methylation. It is important to note that the lowest molecular weight of the MPyMeCh was obtained (Table 3). This is a reason why the high DQ of the MPyMeCh exhibited lower cytotoxicity than the TMChC2 and MDMCMCh1. Similar observations had been reported by Mao et al. (2005) and Kean et al. (2005) who reported that the cytotoxicity of the TMChC increased with increasing molecular weight.

4. Conclusion

The methylation of *N*-aryl chitosan derivatives by a single treatment with iodomethane was successfully synthesized. The thermal stability and crystallinity of the methylated chitosan derivatives were lower than those of chitosan. The mucoadhesive property of methylated *N*-(4-*N*,*N*-dimethylaminocinnamyl) chitosan chloride (MDMCMCh) and methylated *N*-(4-pyridylmethyl) chitosan chloride (MPyMeCh) was as well as *N*,*N*,*N*-trimethylammonium chitosan chloride (TMChC) when the degree of quaterniation (DQ) higher than 65%. However, the mucoadhesive property of the MDMCMCh decreased if the DQ was lower than 65%. Furthermore, it was found the MPyMeChs had a mucoadhesive property as well as TMChC at similar the DQ level even their molecular weight were lower than that of TMChC. The cytotoxicity of methylated chitosan derivatives increased with increasing DQ. It was noted that the MDMCMCh showed the highest cytotoxicity compared to other methylated chitosan derivatives at similar the DQ level. In summary, the effect of the DQ and polymer structure on the mucoadhesive property was obviously when DQ higher than 65%. Therefore, the DQ and the polymer structure played an important role on mucoadhesive property while the cytotoxicity correlated with DQ, the polymer structure, positive charge location and molecular weight after methylation.

Acknowledgements

We gratefully acknowledge the financial support from the Research through National Nanotechnology Center (NANOTEC), National Science and Technology Development Agency (NSTDA), Thailand (Project No. NN-B-22-EN4-94-51-10).

References

Crini, G., Torri, G., Guerrini, M., Morcellet, M., Weltrowski, M., & Martel, B. (1997). NMR characterization of *N*-benzyl sulfonated derivatives of chitosan. *Carbohydrate Polymers, 33*, 145–151.
Ferrari, F., Rossi, S., Bonferoni, M. C., Caramella, C., & Karlsen, J. (1997). Characterization of rheological and mucoadhesive properties of three grades of chitosan hydrochloride. *Farmaco, 52*, 493–497.
Jintapattanakit, A., Mao, S., Kissel, T., & Junyaprasert, V. B. (2008). Physicochemical properties and biocompatibility of *N*-trimethyl chitosan: Effect of quaternization and dimethylation. *European Journal of Pharmaceutics and Biopharmaceutics, 70*, 563–571.
Kean, T., Roth, S., & Thanou, M. (2005). Trimethylated chitosans as non-viral gene delivery vectors: Cytotoxicity and transfection efficiency. *Journal of Controlled Release, 103*, 643–653.
Lai, S. K., Wang, Y. Y., Wirtz, D., & Hanes, J. (2009). Micro- and macrorheology of mucus. *Advanced Drug Delivery Reviews, 61*, 86–100.
Lavertu, M., Xia, Z., Serreqi, A. N., Berrada, M., Rodrigues, A., Wang, D., et al. (2003). A validated ^{1}H NMR method for the determination of the degree of deacetylation of chitosan. *Journal of Pharmaceutical and Biomedical Analysis, 32*, 1149–1158.
Mao, S., Shuai, X., Unger, F., Wittmar, M., Xie, X., & Kissel, T. (2005). Synthesis, characterization and cytotoxicity of poly(ethylene glycol)-graft-trimethyl chitosan block copolymers. *Biomaterials, 26*, 6343–6356.
Muzzarelli, R. A. A., & Tanfani, F. (1985). The *N*-permethylation of chitosan and the preparation of *N*-trimethyl chitosan iodide. *Carbohydrate Polymers, 5*, 297–307.
Polnok, A., Borchard, G., Verhoef, J. C., Sarisuta, N., & Junginger, H. E. (2004). Influence of methylation process on the degree of quaternization of *N*-trimethyl chitosan chloride. *European Journal of Pharmaceutics and Biopharmaceutics, 57*, 77–83.
Qaqish, R. B., & Amiji, M. M. (1999). Synthesis of a fluorescent chitosan derivatives and its application for the study of chitosan–mucin interactions. *Carbohydrate Polymers, 38*, 99–107.
Rossi, S., Ferrari, F., Bonferoni, M. C., & Caramella, C. (2000). Characterization of chitosan hydrochloride-mucin interaction by means of viscosimetric and turbidimetric measurements. *European Journal of Pharmaceutical Sciences, 10*, 251–257.
Rossi, S., Ferrari, F., Bonferoni, M. C., & Caramella, C. (2001). Characterization of chitosan hydrochloride-mucin rheological interaction: influence of polymer concentration and polymer:mucin weight ratio. *European Journal of Pharmaceutical Sciences, 12*, 479–485.
Sajomsang, W., Gonil, P., & Saesoo, S. (2009). Synthesis and antibacterial activity of methylated *N*-(4-*N*,*N*-dimethylaminocinnamyl) chitosan chloride. *European Polymer Journal, 45*, 2319–2328.
Sajomsang, W., Tantayanon, S., Tangpasuthadol, V., & Daly, W. H. (2008). Synthesis of methylated chitosan containing aromatic moieties: Chemoselectivity and effect on molecular weight. *Carbohydrate Polymers, 72*, 740–750.
Sandri, G., Rossi, S., Bonferoni, M. C., Ferrari, F., Zambito, Y., Di Colo, G., et al. (2005). Buccal penetration enhancement properties of *N*-trimethyl chitosan: Influence of quaternization degree on absorption of a high molecular weight molecule. *International Journal of Pharmaceutics, 297*, 146–155.
Shogren, R., Gerken, T. A., & Jentoft, N. (1989). Role of glycosylation on the conformation and chain dimensions of O-linked glycoproteins: Light-scattering studies of ovine submaxillary mucin. *Biochemistry, 28*, 5525–5536.
Sieval, A. B., Thanou, M., Kotze, A. F., Verhoef, J. C., Brussee, J., & Junginger, H. E. (1998). Preparation and NMR characterization of highly substituted trimethyl chitosan chloride. *Carbohydrate Polymers, 36*, 157–165.
Snyman, D., Hamman, J. H., & Kotze, A. F. (2003). Evaluation of the mucoadhesive properties of *N*-trimethyl chitosan chloride. *Drug Development and Industrial Pharmacy, 29*, 61–69.
Sogias, I. A., Williams, A. C., & Khutoryanskiy, V. V. (2008). Why is chitosan mucoadhesive? *Biomacromolecules, 9*, 1837–1842.
Takeuchi, H., Thongborisute, J., Matsui, Y., Sugihara, H., Yamamoto, H., & Kawashima, Y. (2005). Novel mucoadhesion tests for polymers and polymer-coated particles to design optimal mucoadhesive drug delivery systems. *Advanced Drug Delivery Reviews, 57*, 1583–1594.
Wang, Y. Z., Zheng, J. H., Bao, D. C., Lin, J. Z., Sun, Z. J., Liu, X. D., et al. (2007). Mucoadhesive property of chitosan. *Journal of Clinical Rehabilitative Tissue Engineering Research, 11*, 5140–5143.
Zhang, H., & Neau, S. H. (2001). In vitro degradation of chitosan by a commercial enzyme preparation effect of molecular weight and degree of deacetylation. *Biomaterials, 22*, 1653–1658.